

# Universe's Worth of Electrons to Probe Long-Range Interactions of High-Energy Astrophysical Neutrinos

Mauricio Bustamante<sup>1,\*</sup> and Sanjib Kumar Agarwalla<sup>2,3,4,†</sup>

<sup>1</sup>Niels Bohr International Academy and Discovery Center, Niels Bohr Institute, Blegdamsvej 17, 2100 Copenhagen, Denmark

<sup>2</sup>Institute of Physics, Sachivalaya Marg, Sainik School Post, Bhubaneswar 751005, India

<sup>3</sup>Homi Bhabha National Institute, Anushakti Nagar, Mumbai 400085, India

<sup>4</sup>International Centre for Theoretical Physics, Strada Costiera 11, 34151 Trieste, Italy



(Received 27 September 2018; revised manuscript received 9 January 2019; published 12 February 2019)

Astrophysical searches for new long-range interactions complement collider searches for new short-range interactions. Conveniently, neutrino flavor oscillations are keenly sensitive to the existence of long-ranged flavored interactions between neutrinos and electrons, motivated by lepton-number symmetries of the standard model. For the first time, we probe them using TeV-PeV astrophysical neutrinos and accounting for all large electron repositories in the local and distant Universe. The high energies and colossal number of electrons grant us unprecedented sensitivity to the new interaction, even if it is extraordinarily feeble. Based on IceCube results for the flavor composition of astrophysical neutrinos, we set the ultimate bounds on long-range neutrino flavored interactions.

DOI: 10.1103/PhysRevLett.122.061103

**Introduction.**—Are there fundamental interactions whose range is macroscopic but finite? New interactions with ranges of up to 1 A.U. are severely constrained [1–6]: They are feeble at best, so testing for them is tough. Still, searches for new long-range interactions vitally complement collider searches for new short-range interactions.

We present a novel way to study long-range interactions between neutrinos and electrons. Neutrinos are fitting test particles: In the standard model (SM), they interact only weakly, so the presence of a new interaction could more clearly stand out. By considering interaction ranges up to cosmological scales, we become sensitive to the largest electron repositories in the local and distant Universe: Earth, the Moon, Sun, Milky Way, and cosmological electrons. The collective effect of the colossal number of electrons grants us unprecedented sensitivity even if their individual contribution is feeble.

Symmetries of the SM naturally motivate us to consider new neutrino-electron interactions. In the SM, lepton number  $L_l$  ( $l = e, \mu, \tau$ )—the number of leptons minus antileptons of flavor  $l$ —is conserved. So are certain combinations of lepton numbers—among them,  $L_e - L_\mu$  and  $L_e - L_\tau$ . Yet, when treated as broken local symmetries, they introduce a new interaction between electrons  $\nu_e$  and either  $\nu_\mu$  or  $\nu_\tau$  mediated by a new neutral vector boson with undetermined mass and coupling [7–9]. If the boson is light, the range of the interaction is long.

The new interaction affects neutrino oscillations; at high energies, it might drive them. Thus, for the first time, we look for signs of it in the TeV-PeV astrophysical neutrinos seen by IceCube [10–18], whose flavor composition is set by oscillations that occur en route to Earth.

Figure 1 shows that our limits on the new coupling are the strongest for mediator masses under  $10^{-18}$  eV—or

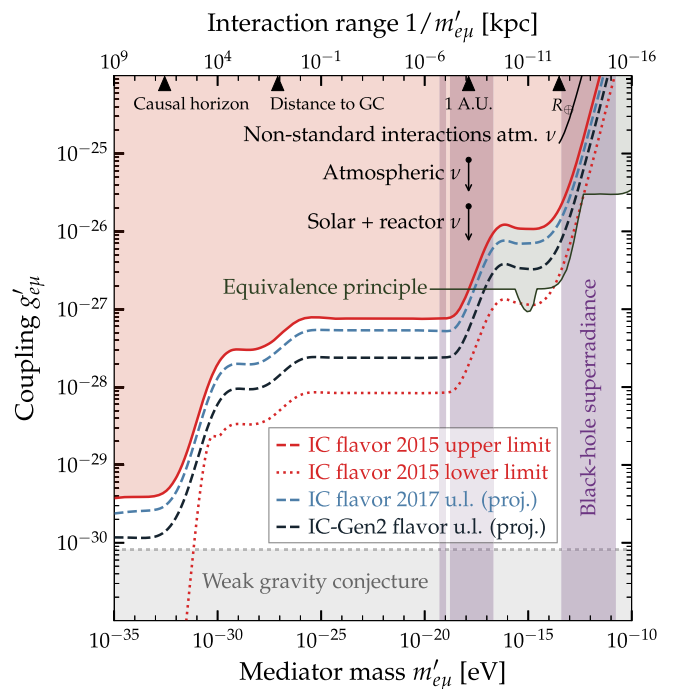


FIG. 1. Constraints on the  $Z'_{e\mu}$  boson mediating long-range neutrino-electron interactions. Our limits come from the flavor composition of high-energy astrophysical neutrinos at  $1\sigma$ , using current IceCube results and projections for IceCube and IceCube-Gen2, assuming normal neutrino mass ordering and a spectrum  $\propto E_\nu^{-2.5}$ . Existing direct limits are from atmospheric [25] and solar and reactor neutrinos [26]. Indirect limits from searches for nonstandard neutrino interactions [27–29] (90% C.L.), tests of the equivalence principle [30] (95% C.L.), and black-hole superradiance [31] (90% C.L.). The weak gravity conjecture [32] suggests that gravity is the weakest force and so  $g_{e\mu}^2 \geq G_N m_\nu^2$ ; we adopt a neutrino mass  $m_\nu = 0.01$  eV.

interaction ranges above 1 A.U. By exploring the parameter space continuously, down to masses of  $10^{-35}$  eV, we improve by orders of magnitude over the reach of previous limits from atmospheric, solar, and reactor neutrino experiments [19–26]. By tapping into a universe’s worth of electrons, we reach the best possible sensitivity.

*Lepton-number symmetries.*—We focus on the lepton-number symmetries  $L_e - L_\mu$  and  $L_e - L_\tau$  of the SM. The related symmetry  $L_\mu - L_\tau$ —which we do not consider here—has been studied extensively as a means to generate a lepton mixing angle  $\theta_{23} \approx 45^\circ$  [33–39]. These are anomaly-free symmetries [7–9]: When promoted to local  $U(1)$  symmetries and broken, they produce some of the simplest extensions of the SM. They only increase the particle content by adding one new neutral vector gauge boson  $Z'_{e\mu}$  or  $Z'_{e\tau}$ . These acquire a mass  $m'_{e\beta} = g'_{e\beta} \langle S_{e\beta} \rangle$  ( $\beta = \mu, \tau$ ) by coupling to a scalar Higgs field with vacuum expectation value  $\langle S_{e\beta} \rangle$  [8,9]. In this prescription,  $L_e - L_\beta$  remain global symmetries, and the undetermined values of  $m'_{e\beta}$  and  $g'_{e\beta}$  can be arbitrarily small.

*Long-range potential.*—Under the  $L_e - L_\beta$  symmetry, a neutrino separated a distance  $d$  from a source of  $N_e$  electrons experiences a Yukawa potential  $V_{e\beta} = g_{e\beta}^2 N_e (4\pi d)^{-1} e^{-d/m'_{e\beta}}$  mediated by the  $Z'_{e\beta}$ . The suppression due to the mediator mass kicks in at distances beyond the interaction range  $1/m'_{e\beta}$ . Thus, for a given value of the mass, the total potential is the aggregated contribution from all electrons located roughly within the interaction range. We explore masses from  $10^{-10}$  to  $10^{-35}$  eV; the associated interaction range varies from meters to  $10^3$  Gpc—much larger than the observable Universe, i.e., effectively infinite. Below, we outline the calculation of the potential; details are in the Supplemental Material [40].

Figure 2 sketches the electron repositories used in our analysis. In the local Universe, the largest repositories of electrons are Earth ( $N_{e,\oplus} \sim 10^{51}$ ), the Moon ( $N_{e,\zeta} \sim 10^{49}$ ), Sun ( $N_{e,\odot} \sim 10^{57}$ ), and the stars and gas of the Milky Way ( $N_{e,MW} \sim 10^{67}$ ). For Earth, we calculate the potential due to electrons in its interior acting on neutrinos that reach the detector from all directions, each traversing a different electron column density inside Earth. For the Moon and the Sun, we take them as point sources of electrons at distances of  $d_\zeta \approx 4 \times 10^5$  km and  $d_\odot = 1$  A.U. For the Milky Way, we compute the potential at the position of Earth—8 kpc from the Galactic Center (GC)—due to all known Galactic baryonic matter. We adopt a sophisticated model of the Galaxy that includes the central bulge, thin disk, and thick disk of stars and cold gas [45], and the diffuse halo of hot gas [46].

In addition, there is a cosmological contribution, previously overlooked, from  $N_{e,\text{cos}} \sim 10^{79}$  electrons contained inside the causal horizon [47], i.e., the largest causally connected region centered on the neutrino. We gain sensitivity to these electrons when the interaction range

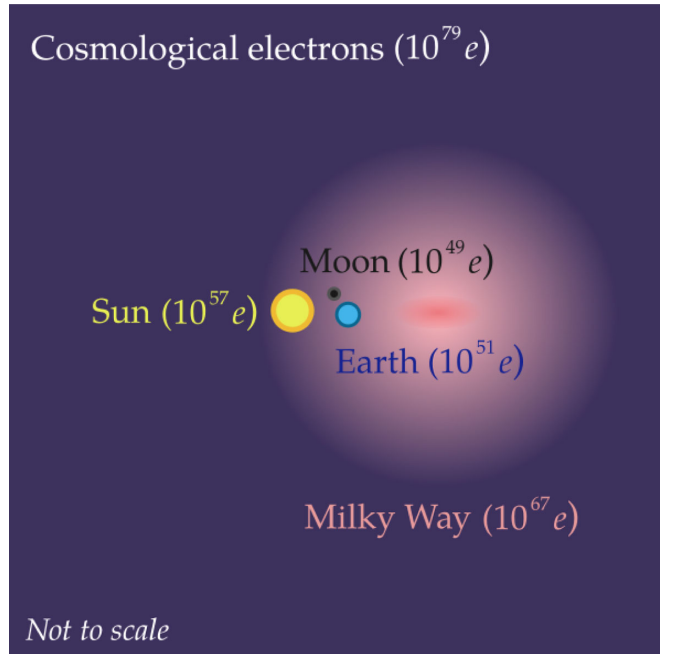


FIG. 2. Electron repositories in the local and distant Universe used to set limits on long-range neutrino-electron interactions.

is of Gpc-scale or larger. Since the number density of cosmological electrons changes as the Universe expands, we compute a redshift-averaged potential due to them, weighed by the number density  $\rho_{\text{SRC}}$  of neutrino sources:  $\langle V_{e\beta}^{\text{cos}} \rangle \propto \int dz \rho_{\text{SRC}}(z) dV_c / dz V_{e\beta}^{\text{cos}}(z)$ , where  $V_{e\beta}^{\text{cos}}(z)$  is the potential at redshift  $z$  and  $V_c$  is the comoving volume [48]. Because astrophysical neutrinos are largely extragalactic in origin [49], we reasonably assume that  $\rho_{\text{SRC}}$  follows the star formation rate [50–52].

Figure 3 shows the total potential  $V_{e\beta} = V_{e\beta}^\oplus + V_{e\beta}^\zeta + V_{e\beta}^\odot + V_{e\beta}^{\text{MW}} + \langle V_{e\beta}^{\text{cos}} \rangle$  as a function of the mediator mass and coupling. Tracing the isocontour of constant  $V_{e\beta}$  from high to low masses reveals the transitions that the potential undergoes as the interaction range grows. From  $10^{-10}$  to  $10^{-18}$  eV, the potential is sourced mainly by Earth and, to a lesser degree, the Moon. The sharp jump at  $1/m'_{e\beta} = R_\oplus$  is due to standard Earth matter effects turning on. At  $10^{-18}$  eV, the interaction range reaches the Sun, the potential receives the contribution of solar electrons, and the isocontour jumps to a lower value of the coupling. At progressively smaller masses, the interaction range grows, and the potential receives the aggregated contribution from electrons distributed in the Milky Way. At  $10^{-27}$  eV, the interaction range reaches the GC, and the isocontour jumps to an even lower value of the coupling, since the GC contains more electrons. Finally, at  $5 \times 10^{-33}$  eV, the interaction range reaches the size of the causal horizon, and the potential is saturated by all of the electrons in the observable Universe.

*Flavor transitions.*—The new interaction affects the evolution of flavor as neutrinos propagate. The evolution

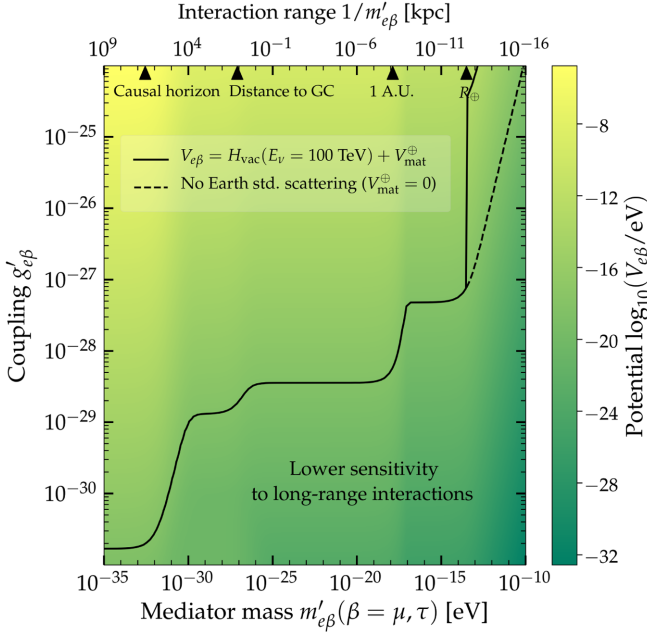


FIG. 3. Long-range potential  $V_{e\beta}$  induced by the  $L_e - L_\beta$  symmetry ( $\beta = \mu, \tau$ ) sourced by electrons in Earth, the Moon, Sun, Milky Way, and by cosmological electrons. The  $Z'_{e\beta}$  boson that mediates the potential has mass  $m'_{e\beta}$  and coupling  $g'_{e\beta}$ . The curve is the isocontour of the potential at a value the vacuum oscillation Hamiltonian—concretely, its element  $H_{vac,ee}$ —evaluated at  $E_\nu = 100$  TeV, plus the potential  $V_{mat}^\oplus$  due to standard matter effects inside Earth. Because of the  $\sim 1/E_\nu$  dependence of  $\mathbf{H}_{vac}$  and the  $\sim g_{e\beta}^2$  dependence of  $V_{e\beta}$ , the isocontour would shift to lower couplings at higher  $E_\nu$ .

is described by the Hamiltonian  $\mathbf{H}_{e\beta} = \mathbf{H}_{vac} + \mathbf{V}_{e\beta} + \Theta(R_\oplus - m'_{e\beta})\mathbf{V}_{mat}^\oplus$ , here written in the flavor basis. The first term accounts for vacuum oscillations:  $\mathbf{H}_{vac} = (2E_\nu)^{-1}\mathbf{U}\mathbf{M}^2\mathbf{U}^\dagger$ , where  $E_\nu$  is the neutrino energy,  $\mathbf{M}^2 = \text{diag}(0, \Delta m_{21}^2, \Delta m_{31}^2)$ , and  $\mathbf{U}$  is the Pontecorvo-Maki-Nakagawa-Sakata (PMNS) mixing matrix parametrized, as usual, via the mixing angles  $\theta_{12}, \theta_{23}, \theta_{13}$ , and the  $CP$ -violation phase  $\delta_{CP}$ . The second term accounts for the new interaction [19,20,22–26]:  $\mathbf{V}_{e\beta} = \text{diag}(V_{e\beta}, -\delta_{\mu\beta}V_{e\beta}, -\delta_{\tau\beta}V_{e\beta})$ . The third term accounts for standard matter effects inside Earth:  $\mathbf{V}_{mat}^\oplus = \text{diag}(V_{mat}^\oplus, 0, 0)$ , where  $V_{mat}^\oplus \equiv \sqrt{2}G_F n_e^\oplus$ , and  $n_e^\oplus$  is the electron number density; see the Supplemental Material [40] for details. This term is relevant only when the interaction range is smaller than the radius of Earth, i.e., when  $m'_{e\beta} \leq R_\oplus$ . When the new potential or the standard matter potential dominates, the Hamiltonian becomes diagonal and flavor mixing turns off. For antineutrinos,  $\delta_{CP} \rightarrow -\delta_{CP}$ ,  $\mathbf{V}_{e\beta} \rightarrow -\mathbf{V}_{e\beta}$ , and  $\mathbf{V}_{mat}^\oplus \rightarrow -\mathbf{V}_{mat}^\oplus$ .

From here, we compute the probability of the flavor transition  $\nu_\alpha \rightarrow \nu_\beta$ . For high-energy neutrinos, the probability oscillates rapidly with distance—the oscillation length is tiny compared to the propagated distances,

i.e.,  $10^{-10}$  Mpc vs Gpc. Thus, we approximate the probability by its average value [53],  $P_{\alpha\beta}(E_\nu) = \sum_{i=1}^3 |U'_{\alpha i}(E_\nu)|^2 |U'_{\beta i}(E_\nu)|^2$ , where  $\mathbf{U}'$  is the matrix that diagonalizes  $\mathbf{H}_{e\beta}$ . It has the same structure as the PMNS matrix, but its elements depend not only on  $\theta_{12}, \theta_{23}, \theta_{13}$ , and  $\delta_{CP}$ , but also on  $\Delta m_{21}^2, \Delta m_{31}^2, g'_{e\beta}, m'_{e\beta}$ , and  $E_\nu$ . Below, to obtain our results, we numerically compute  $P_{\alpha\beta}$  for each choice of values of these parameters.

*Flavor ratios at the sources.*—We expect high-energy astrophysical neutrinos to be produced in the decay of charged pions made in  $pp$  and  $p\gamma$  collisions, i.e.,  $\pi^+ \rightarrow \mu^+ \nu_\mu \rightarrow e^+ \nu_e \bar{\nu}_\mu \nu_\mu$  and its charge conjugate. Thus, neutrinos leave the sources with flavor ratios  $(f_{e,S} : f_{\mu,S} : f_{\tau,S}) = (\frac{1}{3} : \frac{2}{3} : 0)$ . In the main text, we derive limits using this nominal expectation for  $f_{\alpha,S}$ . In the Supplemental Material [40], we consider the alternative “muon-damped” case  $(0 : 1 : 0)_S$ , which might occur at  $E_\nu \gtrsim 1$  PeV if secondary muons lose energy via synchrotron radiation before decaying so that high-energy neutrinos come only from the direct decay of pions. Our conclusions are unaffected by this choice. In Fig. 4, in addition to these two cases, we show only for illustration the case  $(1 : 0 : 0)_S$ —a pure- $\nu_e$  flux coming, e.g., from neutron decay.

*Flavor ratios at Earth.*—At Earth, due to mixing, the ratios become  $f_{\alpha,\oplus} = \sum_{\beta=e,\mu,\tau} P_{\beta\alpha} f_{\beta,S}$ . Under standard mixing, i.e., if  $V_{e\beta}$  is zero, the ratios at Earth are approximately  $(\frac{1}{3} : \frac{1}{3} : \frac{1}{3})_\oplus$ . If  $V_{e\beta}$  is nonzero, the ratios at Earth depend on  $g'_{e\beta}$  and  $m'_{e\beta}$ . Since the vacuum contribution to mixing scales  $\propto 1/E_\nu$ , at the energies recorded by IceCube it might be subdominant, making flavor ratios sensitive probes of new physics [57–85].

We adopt the likely scenario [86,87] in which the flux consists of equal parts of  $\nu$  and  $\bar{\nu}$ , as expected from neutrino production via  $pp$  collisions [88]. At Earth, the flavor ratios are calculated by averaging over  $\nu$  and  $\bar{\nu}$ , since IceCube cannot distinguish between them.

Figure 4 shows how the flavor ratios at Earth vary with the potential. When the potential is small, the flavor ratios are contained inside the small region expected from standard mixing [57]. When the potential is large, mixing turns off and the flavor composition exits the “theoretically palatable region” accessible by standard mixing [57]. In between, the wiggles in the flavor ratios are due to a new resonance in the mixing parameters driven by the long-range potential; see the Supplemental Material [40].

*Flavor ratios in IceCube.*—In IceCube, TeV-PeV astrophysical neutrinos [10–18] scatter off nucleons; scattered charged particles shower and radiate Cherenkov light that is collected by photomultipliers. In general, it is not possible to identify flavor on an event-by-event basis [57,71,89], but it is possible to infer the flavor ratios of the astrophysical flux by comparing relative numbers of different event classes [16,67,71,72,77,90].

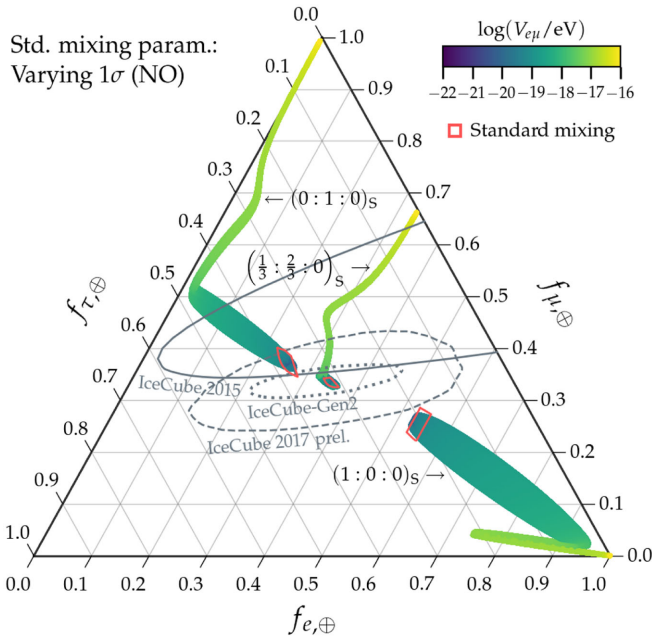


FIG. 4. Flavor ratios at Earth  $f_{\alpha, \oplus}$  as functions of the long-range potential  $V_{e\mu}$  associated to the  $L_e - L_\mu$  symmetry for three illustrative choices of flavor ratios at the sources  $(f_{e,S} : f_{\mu,S} : f_{\tau,S}) = (\frac{1}{3} : \frac{2}{3} : 0)$  (nominal case),  $(0 : 1 : 0)$  (shown in the Supplemental Material [40]) and  $(1 : 0 : 0)$  (pure  $\nu_e$  from neutron decay shown only for illustration). We assume equal fluxes of  $\nu$  and  $\bar{\nu}$ . In this plot, neutrino energy is fixed at  $E_\nu = 100$  TeV for illustration, but our limits are obtained using energy-averaged flavor ratios  $\langle f_{\alpha, \oplus} \rangle$  (see main text), which behave similarly to  $V_{e\beta}$ . For every value of  $V_{e\mu}$ , we scan over values of the standard-mixing parameters within their  $1\sigma$  ranges [54] under normal ordering (NO). We include the IceCube  $1\sigma$  flavor contours that we use to set limits on the new interaction: the current one [16] (“IceCube 2015”) and projections for IceCube [55] (“IceCube 2017”) and IceCube-Gen2 [56,57]. For comparison, we show the regions of  $f_{\alpha, \oplus}$  allowed by standard mixing at  $1\sigma$ .

Figure 4 shows the latest published IceCube flavor results at  $1\sigma$  C.L. [16]; the best-fit composition is  $(0.49 : 0.51 : 0)_{\oplus}$ . Presently, the nominal expectation  $(\frac{1}{3} : \frac{1}{3} : \frac{1}{3})_{\oplus}$  is  $\sim 1\sigma$  removed from the best fit [16]. Below, we explore also projections where the IceCube best-fit point moves closer to the nominal expectation. At confidence levels higher than  $1\sigma$ , present IceCube contours are significantly wider [16]. Present IceCube results disfavor a scenario without oscillations—where  $f_{\alpha, \oplus} = f_{\alpha, S}$ —at  $\sim 1\sigma$ , which allows us to constrain the new interaction at this level. Figure 4 also shows a preliminary update of the IceCube flavor sensitivity [55] and an estimate [57] for the IceCube-Gen2 upgrade [56]. Both are artificially centered on the nominal expectation for  $f_{\alpha, \oplus}$ .

Before contrasting our flavor predictions with IceCube results, we fold in the neutrino energy spectrum. The incoming flux of  $\nu_\alpha + \bar{\nu}_\alpha$  is  $\Phi_\alpha(E_\nu) \propto f_{\alpha, \oplus}(E_\nu) E_\nu^{-\gamma}$ .

Different analyses yielded different values of the spectral index:  $\gamma = 2.50$  using events of all classes [16] and  $\gamma = 2.13$  using only upward-going muons [18]. Below, we consider these two possibilities; the choice has little effect. The average flux in the interval 25 TeV–2.8 PeV [16], where the IceCube flavor results apply, is  $\langle \Phi_\alpha \rangle \approx (2.8 \text{ PeV})^{-1} \int dE_\nu \Phi_\alpha(E_\nu)$ . From this, we define energy-averaged ratios  $\langle f_{\alpha, \oplus} \rangle \equiv \langle \Phi_\alpha \rangle / \sum_\beta \langle \Phi_\beta \rangle$ , our observables. The behavior of  $\langle f_{\alpha, \oplus} \rangle$  resembles that of  $f_{\alpha, \oplus}$  in Fig. 4.

*Limit-setting procedure.*—To constrain the  $Z'_{e\beta}$ , we compare  $\langle f_{\alpha, \oplus} \rangle$  to the IceCube flavor measurements. This way, the IceCube analysis systematics involved in extracting the flavor ratios are already implicitly taken into account. We describe our procedure below.

For a particular choice of values  $(m'_{e\beta}, g'_{e\beta})$ , we independently vary the standard-mixing parameters  $\theta_{12}, \theta_{23}, \theta_{13}, \delta_{CP}, \Delta m_{21}^2$ , and  $\Delta m_{31}^2$  within their experimentally allowed  $1\sigma$  ranges, on a fine grid. We use the ranges from Ref. [54], assuming a normal neutrino mass ordering, which is currently favored over the inverted one at  $3.5\sigma$  [91]. Later, we comment on the inverted ordering. For each choice of values of the mixing parameters, we compute the energy-averaged ratios  $(\langle f_{e, \oplus} \rangle : \langle f_{\mu, \oplus} \rangle : \langle f_{\tau, \oplus} \rangle)$ . We impose a simple hard cut: If the ratios calculated for all choices of values of the mixing parameters fall outside the  $1\sigma$  IceCube contour, then the point  $(m'_{e\beta}, g'_{e\beta})$  is disfavored at, at least,  $1\sigma$  C.L. Otherwise, the point  $(m'_{e\beta}, g'_{e\beta})$  is allowed. We scan  $m'_{e\beta}$  and  $g'_{e\beta}$  over wide intervals and repeat the above procedure for every value.

We also derive limits based on the projected IceCube and IceCube-Gen2 flavor contours in Fig. 4. Even though by the time of completion of IceCube-Gen2—late 2020s—the mixing parameters should be known to higher precision [92], we have tested that already now their uncertainty is not a limiting factor. Using reduced uncertainties—5% for  $\delta_{CP}$  and 1% for all other parameters—the projected limits are only slightly better.

*Results.*—Figure 1 shows that our limits on the coupling  $g'_{e\mu}$  are the strongest for masses below  $10^{-18}$  eV. The limits on  $g'_{e\tau}$  are similar. They are in the Supplemental Material [40], which contains also the limits for alternative choices.

Using current IceCube flavor results, we can place an upper limit because the no-oscillation point  $(\frac{1}{3} : \frac{2}{3} : 0)_{\oplus}$ —reachable with large couplings—lies outside the IceCube contour; see Fig. 4. We can place a lower limit too because the standard-mixing region—reachable with small couplings—also lies outside the contour.

Figure 1 also shows the limits derived using the projected IceCube and IceCube-Gen2 flavor contours. Both contours fully contain the standard-mixing region but not  $(\frac{1}{3} : \frac{2}{3} : 0)_{\oplus}$ ; see Fig. 4. Hence, in these projections, we can set only upper limits. With IceCube-Gen2, the limits could be 4 times better than the current ones.

Our limits are robust against uncertainties in the shape of the neutrino spectrum and choice of mass ordering. Soft ( $\gamma = 2.50$ ) and hard ( $\gamma = 2.13$ ) spectra yield marginally different limits, since the energy-averaged  $\langle f_{\alpha,\oplus} \rangle$  are dominated by low energies; we show results only for  $\gamma = 2.50$ . For the alternative choice  $(0:1:0)_S$ , the limits improve by a factor of 2.5–5 depending on  $m'_{e\mu}$ . Switching to inverted mass ordering has little effect on the upper limits, since the no-oscillation point still lies outside the  $1\sigma$  flavor contour. However, the lower limits derived using current IceCube flavor results deteriorate, on account of our hard  $1\sigma$  cut, because most of the standard-mixing region now falls inside the IceCube contour, thus, allowing smaller values of the coupling.

Our limits outperform the existing ones. The existing direct limits come from atmospheric [25] and solar and reactor neutrinos [19,26]. The indirect limits come from tests of nonstandard neutrino interactions [27–29]—calculated for Fig. 1 following Ref. [23], but only up to  $m_{e\beta}^{-1} = R_{\oplus}$  and using our long-range potential—tests of the equivalence principle [30] and fifth force [93], black-hole superradiance [31], and stellar cooling [94]. Figure 1 shows the most competitive limits; for a full review, including collider limits at higher masses, see Ref. [23].

*Limitations and improvements.*—The main factor limiting our sensitivity is the uncertainty in flavor measurements. However, it is expected to improve in the near future: A larger neutrino event sample and advances in flavor reconstruction [95] will tighten the IceCube flavor results. This will allow the extracted limits to have a higher statistical significance. New directions in flavor-tagging techniques, e.g., muon and neutron echoes [90], could aid. Proposals to distinguish  $\bar{\nu}$  from  $\nu$  could test our assumption of equal fluxes of each [96–98].

If the relic neutrino background contains equal numbers of  $\nu_e$  and  $\bar{\nu}_e$ , it may partially screen out the long-range potential sourced by distant electrons [25,99–101]. We have not considered this effect in our calculation, but it would exclusively affect the sensitivity to couplings  $g'_{e\beta} \lesssim 10^{-29}$ , i.e., the sensitivity due to cosmological electrons. For those couplings, the distance at which this effect becomes relevant—the Debye length [25]—is roughly a factor of 10 smaller than the interaction range  $1/m'_{e\beta}$  to which we are sensitive, given by the values along the curve in Fig. 3.

*Summary.*—In extending the SM, large-scale neutrino telescopes—IceCube and future IceCube-Gen2 and KM3NeT [102]—provide valuable guidance [103] thanks to their detection of neutrinos with the highest energies. We searched for new long-range neutrino-electron interactions mediated by ultralight mediators, via the flavor composition of high-energy astrophysical neutrinos in IceCube. For the first time, we reached the ultimate sensitivity to these interactions, as a result of using the highest neutrino energies and accounting for the huge

number of electrons in the local and distant Universe. Our results, the strongest to date, disfavor the existence of long-range neutrino-electron interactions, crucially complementing results from collider searches for new short-range interactions.

M. B. is supported by the Danmarks Grundforskningsfond Grant No. 1041811001. S. K. A. is supported by DST/INSPIRE Research Grant No. IFA-PH-12, Department of Science and Technology, India and the Young Scientist Project No. INSA/SP/YSP/144/2017/1578 from the Indian National Science Academy. We thank Atri Bhattacharya, Peter Denton, André de Gouvêa, Yasaman Farzan, Matheus Hostert, Shirley Li, Subhendra Mohanty, and Subir Sarkar for feedback and discussion. This work used resources provided by the High Performance Computing Center at the University of Copenhagen. We acknowledge the use of the PYTHON-TERNARY package by Marc Harper *et al.* to produce ternary plots.

\* mbustamante@nbi.ku.dk

† sanjib@iopb.res.in

- [1] T. D. Lee and C.-N. Yang, Conservation of heavy particles and generalized gauge transformations, *Phys. Rev.* **98**, 1501 (1955).
- [2] L. Okun, Leptons and photons, *Phys. Lett. B* **382**, 389 (1996).
- [3] J. G. Williams, X. X. Newhall, and J. O. Dickey, Relativity parameters determined from lunar laser ranging, *Phys. Rev. D* **53**, 6730 (1996).
- [4] A. D. Dolgov, Long-range forces in the universe, *Phys. Rep.* **320**, 1 (1999).
- [5] E. G. Adelberger, B. R. Heckel, and A. E. Nelson, Tests of the gravitational inverse-square law, *Annu. Rev. Nucl. Part. Sci.* **53**, 77 (2003).
- [6] J. G. Williams, S. G. Turyshev, and D. H. Boggs, Progress in Lunar Laser Ranging Tests of Relativistic Gravity, *Phys. Rev. Lett.* **93**, 261101 (2004).
- [7] X. G. He, G. C. Joshi, H. Lew, and R. R. Volkas, New- $Z'$  phenomenology, *Phys. Rev. D* **43**, R22 (1991).
- [8] X.-G. He, G. C. Joshi, H. Lew, and R. R. Volkas, Simplest  $Z'$  model, *Phys. Rev. D* **44**, 2118 (1991).
- [9] R. Foot, X. G. He, H. Lew, and R. R. Volkas, Model for a light  $Z'$  boson, *Phys. Rev. D* **50**, 4571 (1994).
- [10] M. G. Aartsen *et al.* (IceCube Collaboration), First Observation of PeV-Energy Neutrinos with IceCube, *Phys. Rev. Lett.* **111**, 021103 (2013).
- [11] M. G. Aartsen *et al.* (IceCube Collaboration), Evidence for high-energy extraterrestrial neutrinos at the IceCube detector, *Science* **342**, 1242856 (2013).
- [12] M. G. Aartsen *et al.* (IceCube Collaboration), Search for a diffuse flux of astrophysical muon neutrinos with the IceCube 59-string configuration, *Phys. Rev. D* **89**, 062007 (2014).
- [13] M. G. Aartsen *et al.* (IceCube Collaboration), Observation of High-Energy Astrophysical Neutrinos in Three Years of IceCube Data, *Phys. Rev. Lett.* **113**, 101101 (2014).

- [14] M. G. Aartsen *et al.* (IceCube Collaboration), Atmospheric and astrophysical neutrinos above 1 TeV interacting in IceCube, *Phys. Rev. D* **91**, 022001 (2015).
- [15] M. G. Aartsen *et al.* (IceCube Collaboration), Measurement of the atmospheric  $\nu_e$  spectrum with IceCube, *Phys. Rev. D* **91**, 122004 (2015).
- [16] M. G. Aartsen *et al.* (IceCube Collaboration), A combined maximum-likelihood analysis of the high-energy astrophysical neutrino flux measured with IceCube, *Astrophys. J.* **809**, 98 (2015).
- [17] M. G. Aartsen *et al.* (IceCube Collaboration), Evidence for Astrophysical Muon Neutrinos from the Northern Sky with IceCube, *Phys. Rev. Lett.* **115**, 081102 (2015).
- [18] M. G. Aartsen *et al.* (IceCube Collaboration), Observation and characterization of a cosmic muon neutrino flux from the northern hemisphere using six years of IceCube data, *Astrophys. J.* **833**, 3 (2016).
- [19] M. C. Gonzalez-Garcia, P. C. de Holanda, E. Masso, and R. Z. Funchal, Probing long-range leptonic forces with solar and reactor neutrinos, *J. Cosmol. Astropart. Phys.* **01** (2007) 005.
- [20] A. Samanta, Long-range forces: Atmospheric neutrino oscillation at a magnetized detector, *J. Cosmol. Astropart. Phys.* **09** (2011) 010.
- [21] H. Davoudiasl, H.-S. Lee, and W. J. Marciano, Long-range lepton flavor interactions and neutrino oscillations, *Phys. Rev. D* **84**, 013009 (2011).
- [22] S. S. Chatterjee, A. Dasgupta, and S. K. Agarwalla, Exploring flavor-dependent long-range forces in long-baseline neutrino oscillation experiments, *J. High Energy Phys.* **12** (2015) 167.
- [23] M. B. Wise and Y. Zhang, Lepton flavorful fifth force and depth-dependent neutrino matter interactions, *J. High Energy Phys.* **06** (2018) 053.
- [24] A. Khatun, T. Thakore, and S. K. Agarwalla, Can INO be sensitive to flavor-dependent long-range forces?, *J. High Energy Phys.* **04** (2018) 023.
- [25] A. S. Joshipura and S. Mohanty, Constraints on flavour-dependent long-range forces from atmospheric neutrino observations at Super-Kamiokande, *Phys. Lett. B* **584**, 103 (2004).
- [26] A. Bandyopadhyay, A. Dighe, and A. S. Joshipura, Constraints on flavor-dependent long range forces from solar neutrinos and KamLAND, *Phys. Rev. D* **75**, 093005 (2007).
- [27] G. Mitsuka *et al.* (Super-Kamiokande Collaboration), Study of nonstandard neutrino interactions with atmospheric neutrino data in Super-Kamiokande I and II, *Phys. Rev. D* **84**, 113008 (2011).
- [28] T. Ohlsson, Status of non-standard neutrino interactions, *Rep. Prog. Phys.* **76**, 044201 (2013).
- [29] M. C. Gonzalez-Garcia and M. Maltoni, Determination of matter potential from global analysis of neutrino oscillation data, *J. High Energy Phys.* **09** (2013) 152.
- [30] S. Schlamminger, K. Y. Choi, T. A. Wagner, J. H. Gundlach, and E. G. Adelberger, Test of the Equivalence Principle Using a Rotating Torsion Balance, *Phys. Rev. Lett.* **100**, 041101 (2008).
- [31] M. Baryakhtar, R. Lasenby, and M. Teo, Black hole superradiance signatures of ultralight vectors, *Phys. Rev. D* **96**, 035019 (2017).
- [32] N. Arkani-Hamed, L. Motl, A. Nicolis, and C. Vafa, The string landscape, black holes and gravity as the weakest force, *J. High Energy Phys.* **06** (2007) 060.
- [33] S. Choubey and W. Rodejohann, A flavor symmetry for quasi-degenerate neutrinos:  $L_\mu - L_\tau$ , *Eur. Phys. J. C* **40**, 259 (2005).
- [34] T. Ota and W. Rodejohann, Breaking of  $L_\mu - L_\tau$  flavor symmetry, lepton flavor violation and leptogenesis, *Phys. Lett. B* **639**, 322 (2006).
- [35] J. Heeck and W. Rodejohann, Gauged  $L_\mu - L_\tau$  symmetry at the electroweak scale, *Phys. Rev. D* **84**, 075007 (2011).
- [36] K. Harigaya, T. Igari, M. M. Nojiri, M. Takeuchi, and K. Tobe, Muon  $g-2$  and LHC phenomenology in the  $L_\mu - L_\tau$  gauge symmetric model, *J. High Energy Phys.* **03** (2014) 105.
- [37] W. Altmannshofer, S. Gori, M. Pospelov, and I. Yavin, Quark flavor transitions in  $L_\mu - L_\tau$  models, *Phys. Rev. D* **89**, 095033 (2014).
- [38] J. Heeck, M. Holthausen, W. Rodejohann, and Y. Shimizu, Higgs  $\rightarrow \mu\tau$  in Abelian and non-Abelian flavor symmetry models, *Nucl. Phys.* **B896**, 281 (2015).
- [39] A. Crivellin, G. D'Ambrosio, and J. Heeck, Explaining  $h \rightarrow \mu^\pm \tau^\mp$ ,  $B \rightarrow K^* \mu^+ \mu^-$  and  $B \rightarrow K \mu^+ \mu^- / B \rightarrow Ke^+ e^-$  in a Two-Higgs-Doublet Model with Gauged  $L_\mu - L_\tau$ , *Phys. Rev. Lett.* **114**, 151801 (2015).
- [40] See Supplemental Material at <http://link.aps.org/supplemental/10.1103/PhysRevLett.122.061103> for details on the derivation of the long-range potential, flavor mixing in the presence of the long-range potential, constraints derived on the  $L_e - L_\tau$  symmetry, and the effect on the results of the choice of mass ordering, which includes Refs. [41–44].
- [41] A. M. Dziewonski and D. L. Anderson, Preliminary reference Earth model, *Phys. Earth Planet. Inter.* **25**, 297 (1981).
- [42] K. A. Olive *et al.* (Particle Data Group), Review of particle physics, *Chin. Phys. C* **38**, 090001 (2014).
- [43] P. A. R. Ade *et al.* (Planck Collaboration), Planck 2015 results. XIII. Cosmological parameters, *Astron. Astrophys.* **594**, A13 (2016).
- [44] C. Giunti and C. W. Kim, *Fundamentals of Neutrino Physics and Astrophysics* (Oxford University Press, Oxford, 2007).
- [45] P. J. McMillan, Mass models of the Milky Way, *Mon. Not. R. Astron. Soc.* **414**, 2446 (2011).
- [46] M. J. Miller and J. N. Bregman, The structure of the Milky Way's hot gas halo, *Astrophys. J.* **770**, 118 (2013).
- [47] S. Weinberg, *Cosmology* (Oxford University Press, Oxford, 2008).
- [48] D. W. Hogg, Distance measures in cosmology, [arXiv: astro-ph/9905116](https://arxiv.org/abs/astro-ph/9905116).
- [49] M. G. Aartsen *et al.* (IceCube Collaboration), Constraints on Galactic neutrino emission with seven years of IceCube data, *Astrophys. J.* **849**, 67 (2017).
- [50] A. M. Hopkins and J. F. Beacom, On the normalisation of the cosmic star formation history, *Astrophys. J.* **651**, 142 (2006).
- [51] H. Yuksel, M. D. Kistler, J. F. Beacom, and A. M. Hopkins, Revealing the high-redshift star formation rate with gamma-ray bursts, *Astrophys. J.* **683**, L5 (2008).

- [52] M. D. Kistler, H. Yüksel, J. F. Beacom, A. M. Hopkins, and J. S. B. Wyithe, The star formation rate in the reionization era as indicated by gamma-ray bursts, *Astrophys. J.* **705**, L104 (2009).
- [53] S. Pakvasa, Neutrino flavor goniometry by high energy astrophysical beams, *Mod. Phys. Lett. A* **23**, 1313 (2008).
- [54] P. F. de Salas, D. V. Forero, C. A. Ternes, M. Tortola, and J. W. F. Valle, Status of neutrino oscillations 2018:  $3\sigma$  hint for normal mass ordering and improved  $CP$  sensitivity, *Phys. Lett. B* **782**, 633 (2018).
- [55] M. G. Aartsen *et al.* (IceCube Collaboration), The IceCube neutrino observatory—Contributions to ICRC 2017 Part II: Properties of the atmospheric and astrophysical neutrino flux, [arXiv:1710.01191](https://arxiv.org/abs/1710.01191).
- [56] M. G. Aartsen *et al.* (IceCube Collaboration), IceCube-Gen2: A vision for the future of neutrino astronomy in Antarctica, [arXiv:1412.5106](https://arxiv.org/abs/1412.5106).
- [57] M. Bustamante, J. F. Beacom, and W. Winter, Theoretically Palatable Flavor Combinations of Astrophysical Neutrinos, *Phys. Rev. Lett.* **115**, 161302 (2015).
- [58] G. Barenboim and C. Quigg, Neutrino observatories can characterize cosmic sources and neutrino properties, *Phys. Rev. D* **67**, 073024 (2003).
- [59] T. Kashti and E. Waxman, Flavoring Astrophysical Neutrinos: Flavor Ratios Depend on Energy, *Phys. Rev. Lett.* **95**, 181101 (2005).
- [60] Z.-z. Xing and S. Zhou, Towards determination of the initial flavor composition of ultrahigh-energy neutrino fluxes with neutrino telescopes, *Phys. Rev. D* **74**, 013010 (2006).
- [61] P. Lipari, M. Lusignoli, and D. Meloni, Flavor composition and energy spectrum of astrophysical neutrinos, *Phys. Rev. D* **75**, 123005 (2007).
- [62] S. Pakvasa, W. Rodejohann, and T. J. Weiler, Flavor ratios of astrophysical neutrinos: Implications for precision measurements, *J. High Energy Phys.* **02** (2008) 005.
- [63] A. Esmaili and Y. Farzan, An analysis of cosmic neutrinos: Flavor composition at source and neutrino mixing parameters, *Nucl. Phys.* **B821**, 197 (2009).
- [64] K.-C. Lai, G.-L. Lin, and T. C. Liu, Determination of the neutrino flavor ratio at the astrophysical source, *Phys. Rev. D* **80**, 103005 (2009).
- [65] S. Choubey and W. Rodejohann, Flavor composition of UHE neutrinos at source and at neutrino telescopes, *Phys. Rev. D* **80**, 113006 (2009).
- [66] M. Bustamante, A. M. Gago, and C. Pena-Garay, Energy-independent new physics in the flavour ratios of high-energy astrophysical neutrinos, *J. High Energy Phys.* **04** (2010) 066.
- [67] O. Mena, S. Palomares-Ruiz, and A. C. Vincent, On the Flavor Composition of the High-Energy Neutrino Events in IceCube, *Phys. Rev. Lett.* **113**, 091103 (2014).
- [68] X.-J. Xu, H.-J. He, and W. Rodejohann, Constraining astrophysical neutrino flavor composition from leptonic unitarity, *J. Cosmol. Astropart. Phys.* **12** (2014) 039.
- [69] L. Fu, C. M. Ho, and T. J. Weiler, Aspects of the flavor triangle for cosmic neutrino propagation, *Phys. Rev. D* **91**, 053001 (2015).
- [70] C. Y. Chen, P. S. Bhupal Dev, and A. Soni, Two-component flux explanation for the high energy neutrino events at IceCube, *Phys. Rev. D* **92**, 073001 (2015).
- [71] S. Palomares-Ruiz, A. C. Vincent, and O. Mena, Spectral analysis of the high-energy IceCube neutrinos, *Phys. Rev. D* **91**, 103008 (2015).
- [72] M. G. Aartsen *et al.* (IceCube Collaboration), Flavor Ratio of Astrophysical Neutrinos above 35 TeV in IceCube, *Phys. Rev. Lett.* **114**, 171102 (2015).
- [73] A. Palladino and F. Vissani, The natural parameterization of cosmic neutrino oscillations, *Eur. Phys. J. C* **75**, 433 (2015).
- [74] C. A. Argüelles, T. Katori, and J. Salvado, New Physics in Astrophysical Neutrino Flavor, *Phys. Rev. Lett.* **115**, 161303 (2015).
- [75] I. M. Shoemaker and K. Murase, Probing BSM neutrino physics with flavor and spectral distortions: Prospects for future high-energy neutrino telescopes, *Phys. Rev. D* **93**, 085004 (2016).
- [76] H. Nunokawa, B. Panes, and R. Z. Funchal, How unequal fluxes of high energy astrophysical neutrinos and anti-neutrinos can fake new physics, *J. Cosmol. Astropart. Phys.* **10** (2016) 036.
- [77] A. C. Vincent, S. Palomares-Ruiz, and Olga Mena, Analysis of the 4-year IceCube high-energy starting events, *Phys. Rev. D* **94**, 023009 (2016).
- [78] M. C. Gonzalez-Garcia, M. Maltoni, I. Martinez-Soler, and N. Song, Non-standard neutrino interactions in the Earth and the flavor of astrophysical neutrinos, *Astropart. Phys.* **84**, 15 (2016).
- [79] M. M. Reynoso and O. A. Sampayo, Propagation of high-energy neutrinos in a background of ultralight scalar dark matter, *Astropart. Phys.* **82**, 10 (2016).
- [80] M. Bustamante, J. F. Beacom, and K. Murase, Testing decay of astrophysical neutrinos with incomplete information, *Phys. Rev. D* **95**, 063013 (2017).
- [81] V. Brdar, J. Kopp, and X.-P. Wang, Sterile neutrinos and flavor ratios in IceCube, *J. Cosmol. Astropart. Phys.* **01** (2017) 026.
- [82] K.-C. Lai, W.-H. Lai, and G.-L. Lin, Constraining the mass scale of a Lorentz-violating Hamiltonian with the measurement of astrophysical neutrino-flavor composition, *Phys. Rev. D* **96**, 115026 (2017).
- [83] N. Klop and S. Ando, Effects of a neutrino-dark energy coupling on oscillations of high-energy neutrinos, *Phys. Rev. D* **97**, 063006 (2018).
- [84] R. W. Rasmussen, L. Lechner, M. Ackermann, M. Kowalski, and W. Winter, Astrophysical neutrinos flavored with beyond the Standard Model physics, *Phys. Rev. D* **96**, 083018 (2017).
- [85] Y. Sui and P. S. Bhupal Dev, A combined astrophysical and dark matter interpretation of the IceCube HESE and throughgoing muon events, *J. Cosmol. Astropart. Phys.* **07** (2018) 020.
- [86] K. Murase, M. Ahlers, and B. C. Lacki, Testing the hadronuclear origin of PeV neutrinos observed with IceCube, *Phys. Rev. D* **88**, 121301 (2013).
- [87] K. Murase, D. Guetta, and M. Ahlers, Hidden Cosmic-Ray Accelerators as an Origin of TeV-PeV Cosmic Neutrinos, *Phys. Rev. Lett.* **116**, 071101 (2016).
- [88] S. R. Kelner, F. A. Aharonian, and V. V. Bugayov, Energy spectra of gamma-rays, electrons and neutrinos produced at proton-proton interactions in the very high energy

- regime, *Phys. Rev. D* **74**, 034018 (2006); Erratum, *Phys. Rev. D* **79**, 039901(E) (2009).
- [89] A. Palladino, G. Pagliaroli, F.L. Villante, and F. Vissani, What is the Flavor of the Cosmic Neutrinos Seen by IceCube?, *Phys. Rev. Lett.* **114**, 171101 (2015).
- [90] S.W. Li, M. Bustamante, and J.F. Beacom, Echo technique to distinguish flavors of astrophysical neutrinos, [arXiv:1606.06290](https://arxiv.org/abs/1606.06290).
- [91] P.F. De Salas, S. Gariazzo, O. Mena, C.A. Ternes, and M. Trtola, Neutrino mass ordering in 2018: Global status, *Front. Astron. Space Sci.* **5**, 36 (2018).
- [92] P. Coloma, A. Donini, E. Fernandez-Martinez, and P. Hernandez, Precision on leptonic mixing parameters at future neutrino oscillation experiments, *J. High Energy Phys.* **06** (2012) 073.
- [93] E.G. Adelberger, J.H. Gundlach, B.R. Heckel, S. Hoedl, and S. Schlamminger, Torsion balance experiments: A low-energy frontier of particle physics, *Prog. Part. Nucl. Phys.* **62**, 102 (2009).
- [94] E. Hardy and R. Lasenby, Stellar cooling bounds on new light particles: Plasma mixing effects, *J. High Energy Phys.* **02** (2017) 033.
- [95] M.G. Aartsen *et al.* (IceCube Collaboration), Measurements using the inelasticity distribution of multi-TeV neutrino interactions in IceCube, [arXiv:1808.07629](https://arxiv.org/abs/1808.07629) [*Phys. Rev. D* (to be published)].
- [96] L.A. Anchordoqui, H. Goldberg, F. Halzen, and T.J. Weiler, Neutrinos as a diagnostic of high energy astrophysical processes, *Phys. Lett. B* **621**, 18 (2005).
- [97] A. Bhattacharya, R. Gandhi, W. Rodejohann, and A. Watanabe, The Glashow resonance at IceCube: Signatures, event rates and  $pp$  vs.  $p\gamma$  interactions, *J. Cosmol. Astropart. Phys.* **10** (2011) 017.
- [98] V. Barger, L. Fu, J.G. Learned, D. Marfatia, S. Pakvasa, and T.J. Weiler, Glashow resonance as a window into cosmic neutrino sources, *Phys. Rev. D* **90**, 121301 (2014).
- [99] A.D. Dolgov and G.G. Raffelt, Screening of long-range leptonic forces by cosmic background neutrinos, *Phys. Rev. D* **52**, 2581 (1995).
- [100] S.I. Blinnikov, A.D. Dolgov, L.B. Okun, and M.B. Voloshin, How strong can the coupling of leptonic photons be?, *Nucl. Phys.* **B458**, 52 (1996).
- [101] J.A. Grifols and E. Masso, Neutrino oscillations in the sun probe long-range leptonic forces, *Phys. Lett. B* **579**, 123 (2004).
- [102] S. Adrian-Martinez *et al.* (KM3Net Collaboration), Letter of intent for KM3NeT 2.0, *J. Phys. G* **43**, 084001 (2016).
- [103] M. Ahlers, K. Helbing, and C. Prez de los Heros, Probing particle physics with IceCube, *Eur. Phys. J. C* **78**, 924 (2018).